Roll oscillation modulated turning in dynamic millirobots

Duncan W. Haldane, and Ronald S. Fearing

***Abstract*— As we seek to develop more maneuverable legged robots, we need to understand the dynamics of legged turning in an approachable fashion. In this work, we analyze the dynamic turning motion of a dynamic hexapedal millirobot. We explore a family of phase locked turning gaits where all legs of the robot move at the same speed. These gaits are highly periodic, allowing the vertical height and roll angle of the robot to be approximated by single harmonic sinusoidal functions. We demonstrate that oscillations in height and roll angle determine the robot's turning behavior. The phase between these oscillations (and therefore the turning behavior) was modulated by the phase between the left and right sets of legs. A simple model using compliant leg forces was shown to match turning behavior for a range of 5Hz turning gaits. Based on the finding that roll oscillations are major determinants of turning behavior, we modified the robot to create a new high speed turning gait (forward velocity: 0.4 m/s, turn rate 206°/s).**

I. Introduction

Sprawled hexapods, such as cockroaches, show remarkable stability and maneuverability during dynamic locomotion. This is somewhat at odds with the notion that these attributes are reciprocal to each other when it comes to dynamic legged robots. Jindrich and Full [10] have shown that *B. discoicalis* utilizes its highly articulated legs to generate differential forces and moments leading to turns of up to 156 °/s. Because the cockroach's legs have many articulated degrees of freedom, it can generate these turning impulses by pushing or pulling with any of its six legs, allowing for a wide variety of turning behaviors. For example, research by Sponberg et al. has shown that simply shifting the activation phase of a single muscle (the ventral femoral extensor in *B. discoicalis*) can induce a rapid turn within one stride [20]. These results indicate cockroaches possess far more sensors, actuators and even appendages than are required for steady state locomotion or dynamic maneuvering [5]. Therefore by studying the dynamics of turning, it should be possible to extract principles which will allow dynamic legged robots to turn while minimizing the number of required actuators.

A number of legged robots with many degrees of freedom have demonstrated the ability to turn. Aoi et. al used pattern generating oscillators to synthesize gait parameters for a walking robot [1]. Dynamic robots are desirable for fast running, but maneuvering while running is more challenging than for walking robots. Several running robots with fewer actuators have achieved legged steering with varying degrees of success. Reinstein and Hoffmann generated a series of open loop leg commands for a quadrupedal robot (Puppy II) which led to to several periodic, large-radius turning gaits [18]. The hexapedal family of RHex robots [19][7] uses one motor per leg, allowing for diverse and effective modes of dynamic locomotion [6][12]. The RHex robots turn by modulating the parameters of their leg kinematics (prescribed by the Buehler clock) on a per side basis. The details of this steering controller, and a summary of its energetic effect on locomotion are given in [16], but it is only considered for low speed, $0.5 - 1.1Hz$ locomotion. Several other works make reference to this controller [11] but no analysis is presented on the turning dynamics, perhaps because the effect is largely kinematic at these low speeds.

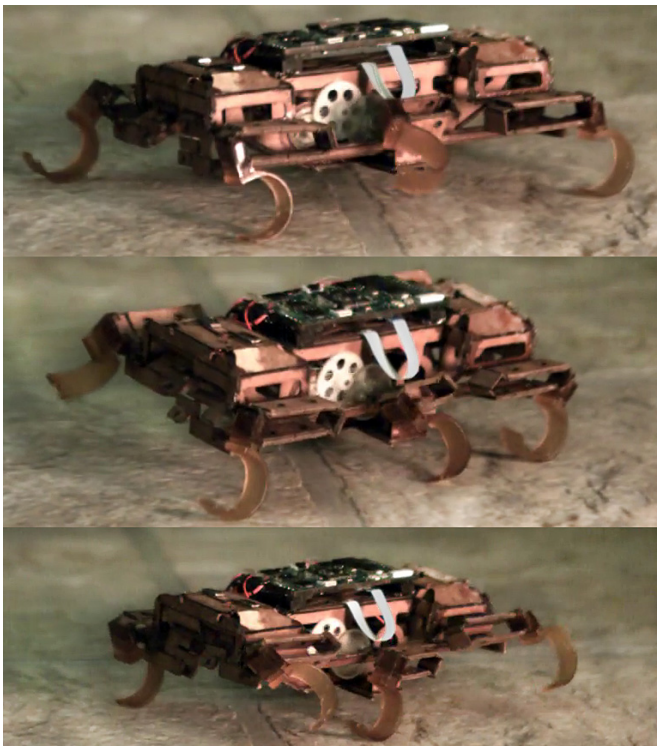

Fig. 1: An image time series showing one half stride of a roll-modulated dynamic turning gait

Extensive research has been performed on the hexapedal Sprawl family of robots as well. The morphology of these robots closely conforms to that of cockroaches, two such versions are, Sprawlette [15] and iSprawl [13]. Sprawlette used six pneumatically powered thrusting legs, each individually mounted on servos which oriented the neutral position of each leg. McClung et al. experimentally characterized the

This material is based upon work supported by the National Science Foundation under IGERT Grant No. DGE-0903711, and Grant No. CNS-0931463, and the United States Army Research Laboratory under the Micro Autonomous Science and Technology Collaborative Technology Alliance.

D.W. Haldane is with the Department of Mechanical Engineering, University of California, Berkeley, CA 94720 USA, *dhaldane@berkeley.edu*

R.S. Fearing is with the Department of Electrical Engineering and Computer Sciences, University of California, Berkeley, CA 94720 USA, *ronf@eecs.berkeley.edu*

turning performance of Sprawlette by adjusting leg thrust angles, and found that increases in turning rate corresponded to significant drops in forward velocity. iSprawl built on the findings of McClung [15] and reduced the number of steering servos down to two, one on each middle leg. iSprawl is capable of making rapid turns, but a dynamic analysis of turning was not reported [13].

Legged millirobots robots are robust and cheap, rapid to manufacture, and rank among the fastest running robots in the world [8]. But they are subject to several constraints such as minimal actuation, and limited control authority, sensing, and processing power. These robots have two or fewer actuators per robot to drive the legs, and rely on kinematic mechanisms to distribute power to the legs. Simple differential velocity steering was shown to be only capable of 100 deg/sec turns in a 10 cm millirobot [17]. Recent work has used an external actuator to achieve steering at high speeds [14], but cockroaches have shown it is possible for a legged system to be highly maneuverable without external actuation. Zarrouk et. al have shown that a hexapedal robot can steer using only one actuator [21].

Our goal is to understand the mechanics of legged turning with robots with very few degrees of freedom. This would help us develop more maneuverable millirobots, and should be extensible to robots of similar morphology with more degrees of freedom. We examine the turning dynamics of a small hexapedal millirobot using phase locked gaits. These gaits were periodic, allowing the underlying mechanics of the turning motion to be easily assessed. In Section II-A we introduce the robotic platform, and the experimental procedure. In Section II-C, we derive simple kinematic equations for predicting turning moment from vertical height, roll angle and leg angle. In Section III we present the mechanics of the turning gaits found in this work. An analysis of the turning gaits is given in Section IV.

II. Methods

A. Experimental procedure

The experimental robotic platform used for this work is the VelociRoACH [8]. This robot is a hexapedal millirobot (shown in Fig. 1) built with cardboard Smart Composite Microstructures [9], making it very cheap to produce. It is 10 cm long, capable of traversing rough terrain, and has a top speed of 2.7 m/s. This robot uses a set of kinematic linkages to drive reciprocating compliant legs using rotary motor motion[1]. There are three legs per side of the robot, with the front and rear legs slaved to be 180° out of phase with the middle leg [8].

For the purpose of this work, it is sufficient to understand that one complete rotation of the motor crank causes the VelociRoACH to take one step with the front and rear legs (with the middle leg off the ground), and then lift them off the ground to step once with the middle leg (detailed descriptions of the kinematics are given in Haldane et al. [8]). The leg angle(ψ) is a function of the motor crank angle(α) involving the relative dimensions of the kinematic linkages. The leg angle is approximated by $\psi = 0.76\cos(\alpha)$. The legs touchdown and liftoff at $\psi = \pm 42^\circ$. In this work we used phase locked, constant speed gaits so the left motor crank angle is simply $\alpha_L = \alpha_R + \Phi_\alpha$, where α_R is the right crank angle, and Φ_α is the relative phase between the two sides.

The VelociRoACH is driven by the ImageProc[2] [2] robot control board. The ImageProc also collects telemetry data at 1000 Hz, and uses a 802.15.4 radio interface for communication and external control[3].

We examined the turning mechanics of several phase locked gaits at 5Hz (the frequency at which the motor crank makes a full rotation). The robot was run for a total of 15 seconds for each phase offset, resulting in 15,000 data points per trial. Externally, the robot was observed by an Optitrack motion tracking system, which collected pose information at 100Hz. The robot ran on a tile surface ($\mu = 0.41$), for these experiments, it was also run on carpet ($\mu = 0.56$) with no observable change in turning behavior.

B. Simplifications and Assumptions

The nonlinear dynamics of this robot are sufficiently complex to preclude straightforward statements about the effect of any individual parameter on the turning behavior of the system. We therefore seek to develop a simplified model which may be less accurate, but will be more accessible in terms of understanding the dynamic mechanisms underlying some turning behaviors.

This simple model assumes bipedal contact, disregarding any potential damping force from the contact of legs dragging on the ground. It also does not take into account any horizontal forces generated by motor torque. The legs are modeled as simple linear springs, neglecting their nonlinear stiffness properties as well as all off axis compliances. These are considerable simplifications, and they affect the forces expected from the robot during stance. However, we expect the dominant forces to act along the length of the leg and proceed with our analysis.

Another major assumption is that pitch oscillations are negligible throughout the stride. As shown in Fig. 2, pitch oscillations have an approximate magnitude of 0.035 radians. If they had a significant effect, these small oscillations would modify the forces applied by the fore and aft legs.

C. Modeling of Leg Forces

We want to find the simplest possible model to understand a the dynamics of legged turning. The z and roll coordinates (along with the crank angle (α)) determine kinematically which legs can touch the ground at any given point in the stride. We expect that these coordinates are the most important determinants for the dynamics of the turning gait. To inspect how z and roll (ϕ) affect turning, we examine the kinematics of the robot, illustrated in Fig. 3a . The right and/or left legs can be on the ground when the following inequalities are satisfied:

[1]The accompanying video best illustrates these mechanisms

[2]Embedded board: https://github.com/biomimetics/imageproc_pcb

[3]Embedded code: https://github.com/dhaldane/roach

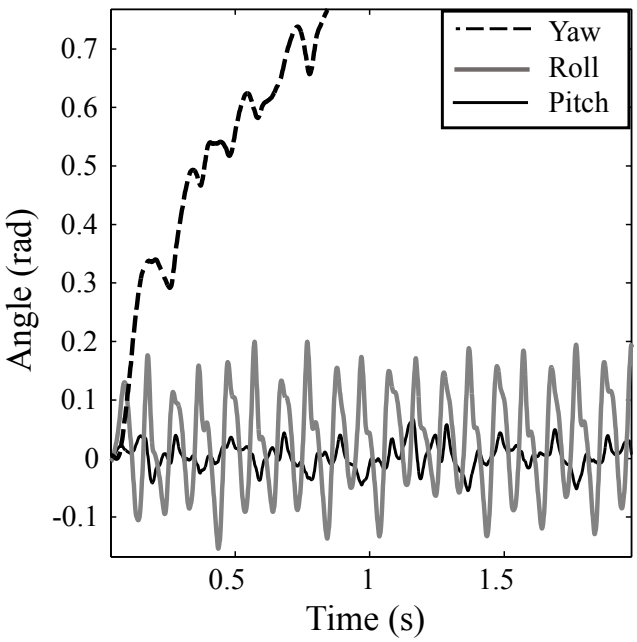

Fig. 2: This plot shows the Euler angles of the robot, as a function of time. Note that the periodic nature of these signals allows them to be minimally represented as compositions of sinusoids. (See Fig. 4)

$$\text{Right: } z \leq \zeta_o \cos(\phi) - \frac{l}{2}\sin(\phi) - z_o \tag{1}$$

$$\text{Left: } z \leq \zeta_o \cos(\phi) + \frac{l}{2}\sin(\phi) - z_o \tag{2}$$

If z and roll are known, then the leg forces can be approximated by finding the leg deflection using a kinematic model. The legs are modeled as simple linear springs with rest length ζ_o and stiffness k (2.25cm and 55N/m, respectively).

The heights of the leg attachment points are:

$$z_R = z_B - \frac{l}{2}\sin(\phi) \qquad z_L = z_B + \frac{l}{2}\sin(\phi), \tag{3}$$

where z_B is the height of the body and l is the width of the robot. The compressed lengths of the legs are then

$$\zeta_R = \min(\zeta_o, \frac{z_R}{\cos(\psi_R)}) \qquad \zeta_L = \min(\zeta_o, \frac{z_L}{\cos(\psi_L)}) \tag{4}$$

where ψ is the angle of the leg. The hybrid state of the leg is dealt with kinematically with the $\min$ function, which simplifies the model. The force vectors are therefore

$$\mathbf{F_R} = k(\zeta_R - \zeta_o)\mathbf{e}_{\zeta_\mathbf{R}} \qquad \mathbf{F_L} = k(\zeta_L - \zeta_o)\mathbf{e}_{\zeta_\mathbf{L}}. \tag{5}$$

where the vector in the direction of the leg is

$$\mathbf{e}_\zeta = \sin(\psi)\mathbf{e_x} - \cos(\psi)\mathbf{e_z}. \tag{6}$$

The net turning moment on the robot, shown in Fig. 3b, is then:

$$M = \frac{l}{2}(\mathbf{F_R}\cdot\mathbf{e_x} - \mathbf{F_L}\cdot\mathbf{e_x}), \tag{7}$$

where $\mathbf{F}\cdot\mathbf{e_x}$ is the horizontal force predicted from the kinematics of the legs. The predicted yaw acceleration is

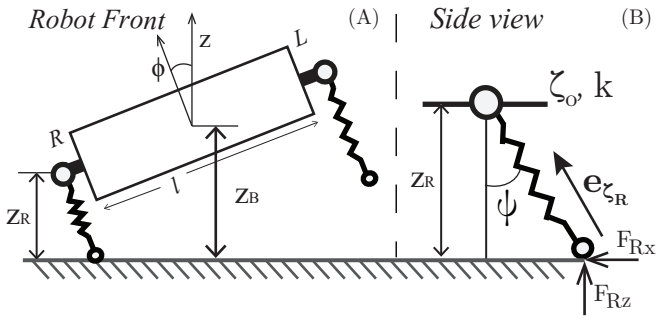

(a) A free body diagram of the robot, showing the effect of z height and roll on the kinematics (A). Leg forces are determined by approximating the leg as a spring and finding the net force given the kinematic variables(B)

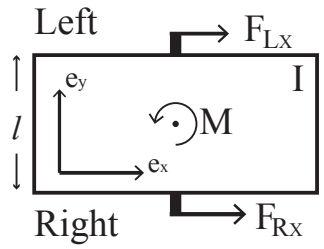

(b) Top view of the robot showing the generation of turning moment M, from leg forces

Fig. 3: Diagrams for deriving leg forces

$\ddot{\psi} = M/I$ where I is the yaw moment of inertia (21.97 kg-mm^2).

The direction of the turning moment the legs apply is a function of the leg angle. If the middle leg is in the first half of stance ($\pi \leq \alpha < \frac{3\pi}{2}$) then the leg applies a braking force, else if the middle leg is in the last half of stance ($\frac{3\pi}{2} \leq \alpha < 2\pi$), the decompressing spring generates a positive force.

III. Turning Mechanics

In this section, the dynamics and turning mechanics of a left-turning gait (5Hz, $\Phi_\alpha = 110°$) will be analyzed. Other gaits using a range of phase offsets (Φ_α) are shown in Section IV, and have similar dynamics.

Our force prediction model relies on knowledge of the z and roll coordinates. Previous work has predicted these coordinates with a detailed hybrid model with hand tuned parameters [4]. As we have data for the robot running and we know it is periodic (Fig. 2), we simply fit sinusoids to the z and roll data. This approach drastically simplifies the model of legged turning, removing the need for a fully descriptive 6 DoF model.

Fig. 4 demonstrates the validity of this approach for modeling oscillations in a 5Hz turning gait. The Fourier spectra in Fig. 4 (A) and (B) show strong peaks at the first, second, and fourth harmonics of the stride frequency. The first and fourth harmonics of the z data are lesser in magnitude and are disregarded for curve fitting. The amplitude(A) and phase(Φ) of these sinusoids were fit to data collected at each tested phase offset using nonlinear regression. Fig. 4(C) and (D), show the fitted sinusoidal approximations. Fig. 4(C) shows

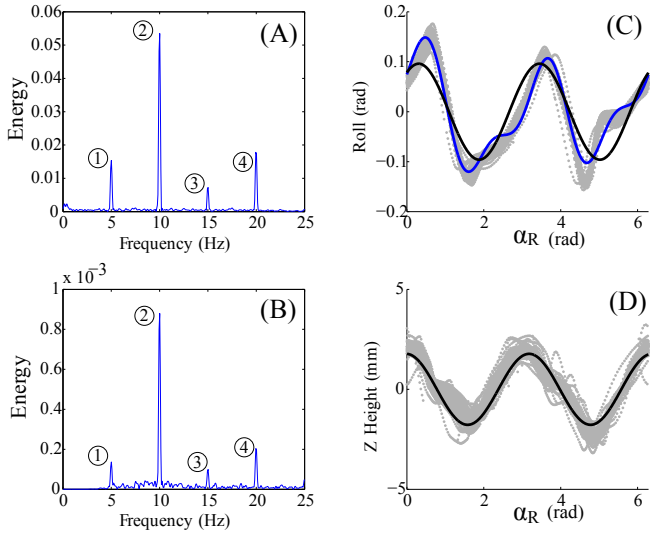

Fig. 4: Fourier spectra of roll (A), and z (B) oscillations during a 5Hz, $\Phi_{alpha} = 110^\circ$ left-turning gait. Note the clear presence of energy on the first, second and fourth harmonics of the stride frequency. These harmonics are labeled with circled numbers. Also shown are time trajectories of the curves fit to the data for roll (C) and z height (D). The blue curve fit to the roll data shows the higher order fit (all three main harmonics), and the black line shows the simplest fit (single largest harmonic).

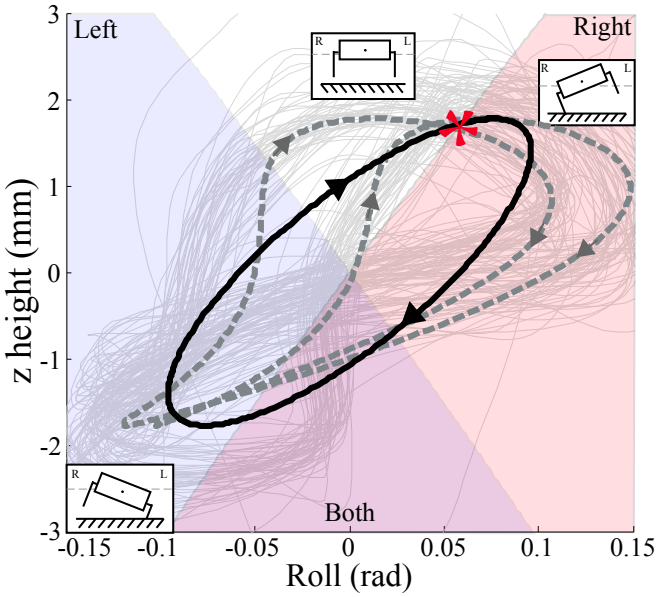

Fig. 5: A plot of the path of the robot on the plane formed by z and ϕ during a 5Hz, $\Phi_\alpha = 110^\circ$ left turning gait. Plotted on top of the experimentally observed data (light gray) are reduced order approximations of the oscillators. The dashed line uses the first, second and fourth harmonic of the stride frequency (there is only a single trajectory). The solid black line uses only the second harmonic, forming an ellipse which traversed twice of the course of a single stride. These sinusoids form Lissajous curves when plotted against each other. Arrows show direction of movement with increasing progress through a stride. The beginning of a stride ($\alpha_R = 0$) is marked with a red asterisk. Cartoons showing the robot from the front are shown to clarify the pose of the robot at different points on the $z - \phi$ plane.

both the approximation made with all significant harmonics (1,2,4), and the reduced approximation made using only the dominant harmonic. By inspecting the fit, we can see that the signal is represented fairly well, but the lower-order approximations appreciably underestimate the amplitude of both signals. This divergence is understandable, because we are approximating a complex hybrid-dynamical system with simple harmonic motion.

To determine the effects of z and roll on the turning dynamics of a legged system, we examine the periodic limit cycle in the $z - \phi$ plane. Fig. 5 shows this trajectory. Shown on this graph are the kinematic bounds of the left and right legs (found from Equations 1,2).

The graph is centered at $(0, 0)$, where the legs of the robot are just touching the ground. The unshaded region of this plot above this point indicates the aerial phase, where no leg is on the ground. In the blue-shaded region, the left leg is in contact with the ground; in the red-shaded region, the right leg can be in contact. These regions overlap in the purple-shaded portion of the graph, indicating the presence of double-stance. The normal distance of a point from the kinematic bounds gives a measure of magnitude of leg loading; i.e. the left leg is highly loaded in the bottom-left portion of the graph, and the right leg would be highly loaded at the bottom-right of the graph. These bounds are also used in Fig. 6. Note that the skew in this graph causes the left leg to be more highly loaded than the right leg.

Plotted on top of the observed trajectory are the reduced order fits found using sinusoidal approximations of the oscillators. When z and roll are approximated using a single harmonic, the path is reduced to a Lissajous curve which is parameterized by the amplitude of the z and roll oscillations and their relative phase. The robot traverses this ellipse twice in the course of one stride. The reduced order approximation underestimates the true amplitude of the oscillations, which diminishes the expected resultant force generated by the compression of the legs.

Fig. 6 shows the resulting Lissajous figures for three different 5 Hz gaits. Fig. 6 (A) is a left turning gait with phase offset $\Phi_\alpha = 110^\circ$, Fig. 6 (B) is a straight running alternating tripod gait with phase offset $\Phi_\alpha = 180^\circ$, and Fig. 6 (C) is a right turning gait with phase offset $\Phi_\alpha = 235^\circ$. There is a symmetry of the leg phase offsets which cause left or right turns about the alternating tripod gait (e.g. $\Phi_\alpha = 180 \pm \approx 65^\circ$). The amplitude of the oscillations stays the same, but adjusting the phase between the legs changes the phase between the z and roll oscillators, from $\delta = 0.65$ for $\Phi_\alpha = 110^\circ$ to $\delta = 2.01$ for $\Phi_\alpha = 235^\circ$. The effect of this change in phase is shown by the Lissajous curves in Fig. 6, and causes the robot to turn opposite from the original direction. In the alternating tripod gait shown in Fig. 6, the dominant roll harmonic is periodic with stride frequency, while the dominant z harmonic is still at twice the stride frequency. This Lissajous curve is not skewed, indicating equal loading on the left and right legs.

Fig. 7 (A) shows the yaw rate of the robot during a left-turning gait, plotted against the crank angle of the right side, α_R. Inspecting the slope of the yaw rate, we find that there

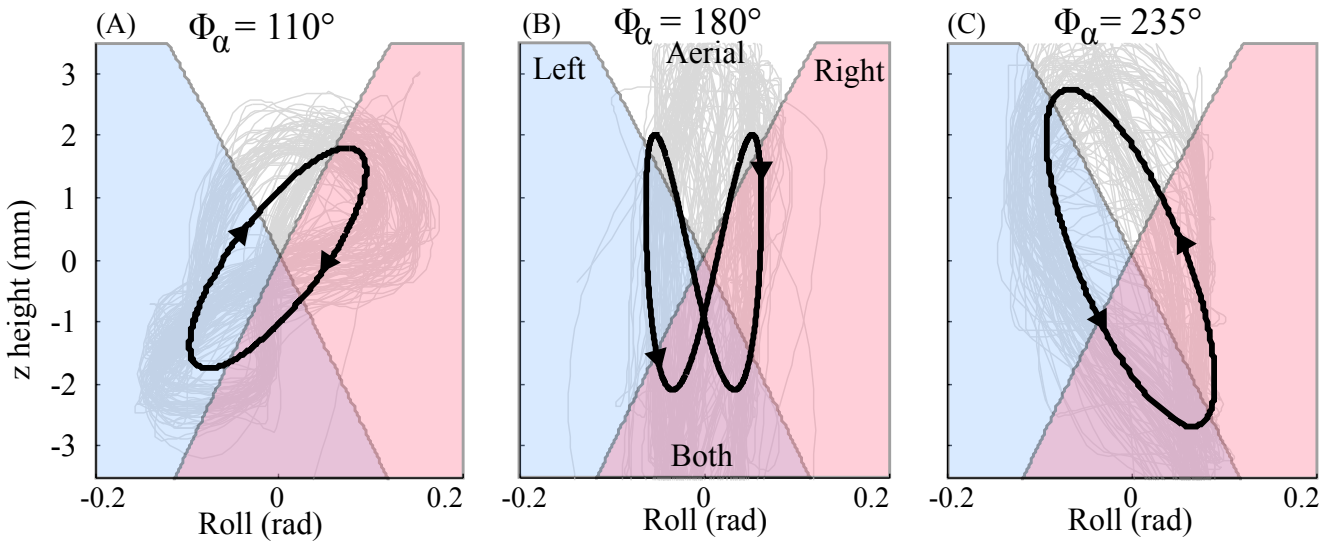

Fig. 6: $z - \phi$ reduced order Lissajous curves for three gaits at 5 Hz. (A) is a left-turning gait with $\Phi_\alpha = 110°$. (B) is the nominally straight alternating tripod gait with $\Phi_\alpha = 180°$. (C) is a right-turning gait with $\Phi_\alpha = 235°$. In both of the turning gaits, the turning is dominated by the braking leg. The shift in the leg phase causes a change in the phase of the $z - \phi$ oscillators, which in turn affects the steering action of the legs.

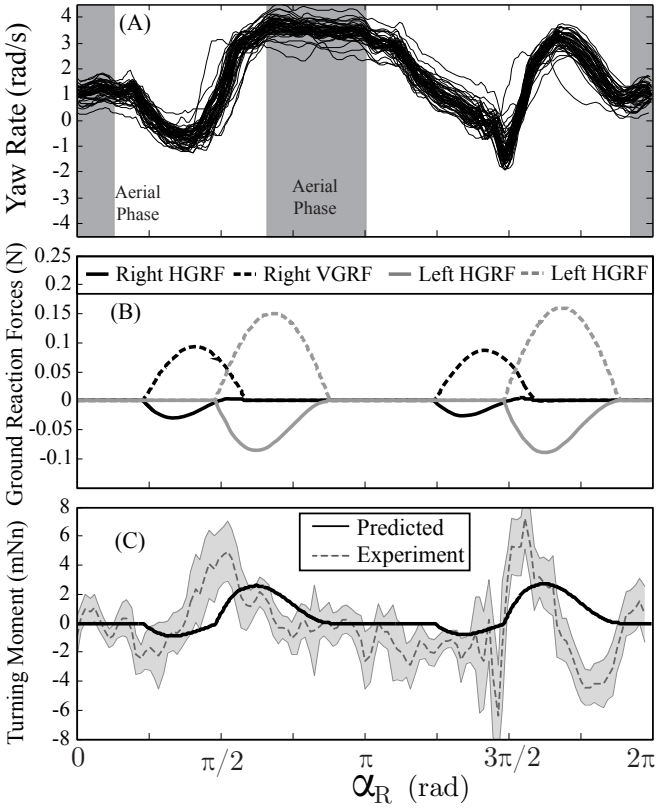

Fig. 7: (A) Yaw rate of the robot while in a left-turning gait. Note the repeated yaw accelerations at $\alpha_R \approx \frac{\pi}{2}$ and $\alpha_L \approx \frac{3\pi}{2}$. (B) Predicted Horizontal (HGRF) and Vertical (VGRF) Ground Reaction Forces. (C) Predicted moment calculated from the estimated ground reaction forces. Also shown is the experimentally observed moment. The measured moment was found by numerically differentiating the z-axis gyroscope, and averaging the result over 50 strides. The shaded area represents one standard deviation. The black lines are the predicted turning moment from the kinematic model prediction of leg forces.

are two points of significant positive yaw acceleration, where the legs of the robot were able to provide a turning moment. These areas of acceleration were only observed to occur when one or both of the middle legs was on the ground, indicating that turning motion for this legged robot is largely dominated by action of the middle legs. The left middle leg applies a braking moment at $\alpha_R \approx \frac{\pi}{2}$, which we expect to be responsible for most of the turning action for several reasons. Firstly, the left leg applies this force when it is highly loaded, (in the bottom-left corner of Fig. 5). Secondly an aerial phase follows the left leg action (shown in Fig. 7 (A), and Fig. 5), where the yaw rate is preserved at its highest positive value.

Fig. 7 (B) shows the prediction of the ground reaction forces using Equation 5. These predictions are made with the simplified models of z and roll which use a single harmonic to approximate the function. The left leg has a large negative ground reaction force, which causes a positive turning moment. These leg forces also show that the right leg is braking the turn. The model under-predicts leg forces from what we expect from this robot, due to the distortion in the estimated $z - \phi$ orbit away from the experimentally observed trajectory.

The turning moment predicted from the leg ground reaction forces (Equation 7) is shown in Fig. 7 (C). Although the ground reaction forces are under predicted with this model, the moment is on the order of that which was observed experimentally.

IV. Results

Fig. 8 shows planar trajectories of the robot running at 5Hz with a range of phase offsets. The robot turns most tightly with a phase offset of $\Phi_\alpha = 110°$, and in circles of increasing diameter at phase offsets of $\Phi_\alpha = 130°$ and $\Phi_\alpha = 150°$. The robot runs in a straight line at $\Phi_\alpha = 180°$, which corresponds to the alternating tripod gait. All of these gaits are repeatable and are open loop stable, retaining a

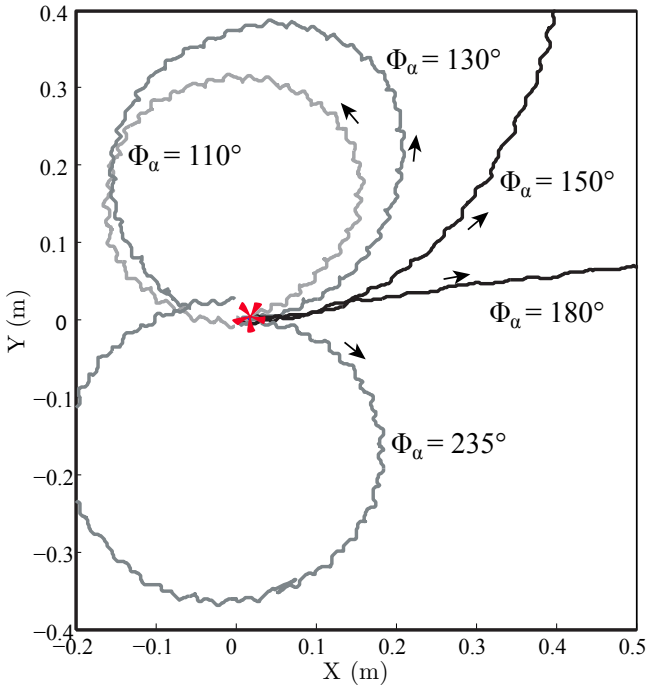

Fig. 8: Position trajectories of phase locked 5Hz gaits. Gaits shown are for left turns, right turns are achieved by reflecting the phase offset Φ_α about the alternating tripod gait. i.e $\Phi_\alpha = 130°$ becomes $\Phi_\alpha = 230°$ for a comparable right turn. All runs begins from (0,0), marked with red asterisk.

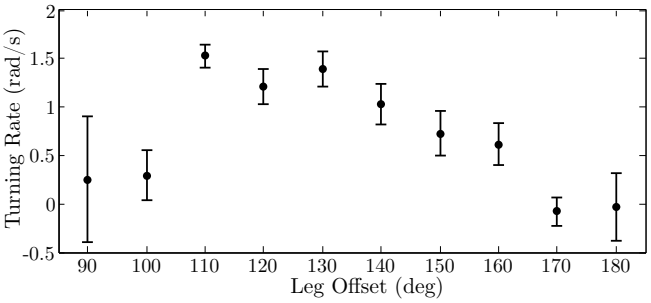

Fig. 9: Turning rate vs leg phase offset for phase locked turning gaits. Error bars show one standard deviation

relatively constant turning rate and speed on a stride averaged basis. The turning direction can be reversed by reflecting the phase offset about $\Phi_\alpha = 180°$ i.e. the $\Phi_\alpha = 235°$ gait is the right turning version of the $\Phi_\alpha = 130°$. The z roll dynamics of three of these gaits are shown in Fig. 6.

The average turning rate as a function of leg phase offset is shown in Fig. 9. These turning gaits are most effective for leg offsets in the range of $\Phi_\alpha = 110° - 130°$. Similar gaits for right turns can be found by reflecting the leg phase offset about 180°. There was no statistically dignificant difference between the power consumption for $\Phi_\alpha = 110°$ and that for straight line running.

Fig. 10 shows measured and predicted turning moments for the left turning (Fig. 10 (A)(B)(C)) and alternating tripod (Fig. 10 (D)) gaits from Fig. 8. A comparison of the measured and predicted turning moments shows how much of the observed turning effect was captured by the simple behavior presented in this work. The model matches most the observed data for Fig. 10 (A), (B) and (C), but underpredicts a deceleration at the end of the stride. This deceleration appears to be caused by the left fore and aft legs dragging on the ground, a feature ignored by the model. The model overpredicts the turning moment for the alternating tripod gait, again this divergence could be explained by fore and aft legs on the ground resisting rotational motion.

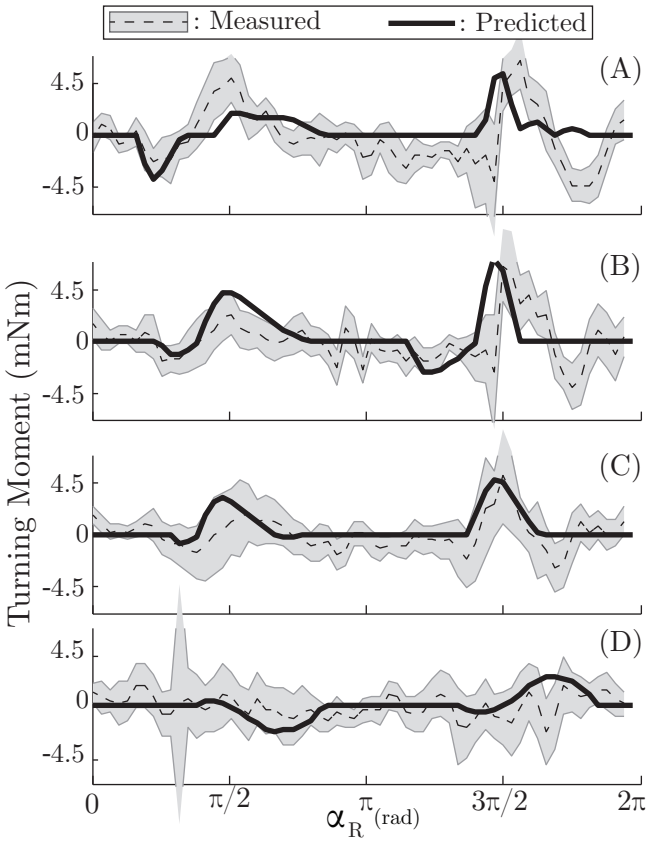

Fig. 10: Measured and predicted turning moments for several 5Hz gaits. (A) $\Phi_\alpha = 110°$, (B) $\Phi_\alpha = 130°$, (C) $\Phi_\alpha = 150°$, (D) $\Phi_\alpha = 180°$. The moments were measured and predicted as in Fig. 7

A. Gait Design

We have established that the z and roll dynamics of a legged robot can largely determine its turning behavior. We therefore sought to enable new high speed turning gaits by modifying the robot's roll dynamics. An appendage was added to the VelociRoACH which increased its roll inertia by a factor of four, effectively halving the natural frequency of roll oscillations. This modification altered the roll dynamics and allowed for the existence of a 8Hz turning gait. This gait was different than the 5Hz gaits in that z and roll became periodic with stride frequency, and the degree of roll oscillation was almost doubled when the extra inertia was added. This roll enabled a rapid turning gait which averaged 3.6 rad/s while traveling at 0.40 m/s.

To compare this performance to that of other robots, we use the maneuverability metric $K = \dot{\psi} v$ where $\dot{\psi}$ is the yaw

rate, and v is the forward velocity. The VelociRoACH, using the turning gaits discovered in this work, is compared to other similar robots in Table I. These new turning gaits are stable and periodic, and allow remarkable maneuverability, especially considering the underactuated nature of the robotic platform.

TABLE I: COMPARISON OF LEGGED TURNING PERFORMANCE

	Robot	# Legs	# Actuators	$K = \dot{\psi} v (^\circ m s^{-2})$
Prior Art	OctoRoACH [17]	8	2	36.0
	X-RHex [16]	6	6	1.44
	iSprawl [13]	6	3	18.0
	SailRoACH [14]	6	3	134
This Work	5Hz Turning	6	2	29.1
	8Hz Turning	6	2	82.5

V. CONCLUSION

In this work we demonstrated a dynamic mechanism for legged turning which depended on inherent z and roll dynamics affecting the forces applied to the robot's compliant legs. The turning behavior of the robot matched predictions made using the leg forces for a range of 5Hz turning gaits. These predictions relied on several strong assumptions which do not hold for the entirety of the robot's operational zone. We therefore conclude that several turning gaits use the dynamic turning mechanism that we identified, but that it does not globally match all turning dynamics for this robot.

The family of dynamic turning gaits in this work drove the legs at the same speed with a simple phase offset between the two sides of the robot. As opposed to using differential steering [17][3] to turn, these gaits were highly periodic and repeatable and among the most maneuverable for similar hexapedal robots (see Table I). The periodic nature of these gaits resembled that of straight line running, and the most effective turning gait did not use more power than simple running. For any phase offset, at stride frequencies corresponding to walking (1-3Hz), the robot did not turn. This led us to conclude the turning effect was a dynamic one, dominated by an interplay of kinetic and potential energy.

Building on the finding that the z and roll dynamics are the main determinants of the turning properties of a phase locked gait, we sought to enable high speed turning. Phase locked gaits were less effective for the unmodified robot as the stride frequency approached that of the roll resonant frequency (11Hz). We modified the robot by adding an appendage which increased the roll inertia, thereby allowing a new turning gait at 8 Hz. The model for the turning mechanism present in the 5Hz gaits did not match the 8Hz case well, indicating that other factors than forces along the length of the leg were contributing to the turning action.

The space of dynamic maneuvers of which legged robots are capable is wide and varied. This work explored a part of that small space and identified a new mechanism for legged turning. Future work should explore this space and boost the agility of legged robots with new dynamic behaviors.

ACKNOWLEDGMENTS

Thanks to the members of the Biomimetic Millisystems Lab for their helpful comments and discussions.

REFERENCES

[1] S. Aoi and K. Tsuchiya, "Adaptive behavior in turning of an oscillator-driven biped robot," *Autonomous Robots*, vol. 23, no. 1, pp. 37–57, May 2007.

[2] S. S. Baek, F. L. Garcia Bermudez, and R. S. Fearing, "Flight control for target seeking by 13 gram ornithopter," *2011 IEEE/RSJ Int. Conf. on Intelligent Robots and Systems*, pp. 2674–2681, Sep. 2011.

[3] A. D. Buchan, D. W. Haldane, and R. S. Fearing, "Automatic identification of dynamic piecewise affine models for a running robot," *2013 IEEE/RSJ International Conference on Intelligent Robots and Systems*, pp. 5600–5607, Nov. 2013.

[4] S. Burden, J. E. Clark, J. D. Weingarten, H. Komsuoglu, and D. E. Koditschek, "Heterogeneous Leg Stiffness and Roll in Dynamic Running," *IEEE Int.Conf. on Robotics and Automation*, pp. 4645–4652, Apr. 2007.

[5] R. J. Full, T. Kubow, J. Schmitt, P. J. Holmes, and D. E. Koditschek, "Quantifying dynamic stability and maneuverability in legged locomotion." *Integrative and comparative biology*, vol. 42, no. 1, pp. 149–57, Mar. 2002.

[6] K. C. Galloway, J. E. Clark, M. Yim, and D. E. Koditschek, "Experimental Investigations into the Role of Passive Variable Compliant Legs for Dynamic Robotic Locomotion," in *IEEE Int. Conf. on Robotics and Automation*, 2011, pp. 1243–1249.

[7] K. C. Galloway, A. M. Johnson, B. Plotnick, R. Knopf, M. White, and D. E. Koditschek, "X-RHex : A Highly Mobile Hexapedal Robot for Sensorimotor Tasks," University of Pennsylvania, Tech. Rep., 2010.

[8] D. W. Haldane, K. C. Peterson, F. L. Garcia Bermudez, and R. S. Fearing, "Animal-inspired Design and Aerodynamic Stabilization of a Hexapedal Millirobot," *IEEE Int. Conf. on Robotics and Automation*, 2013.

[9] A. M. Hoover and R. S. Fearing, "Fast scale prototyping for folded millirobots," *IEEE Int. Conf. on Robotics and Automation*, pp. 886–892, 2008.

[10] D. L. Jindrich and R. J. Full, "Many-legged maneuverability: dynamics of turning in hexapods," *The Journal of experimental biology*, vol. 202 (Pt 12, pp. 1603–23, Jun. 1999.

[11] A. M. Johnson, M. T. Hale, G. C. Haynes, and D. E. Koditschek, "Autonomous legged hill and stairwell ascent," *2011 IEEE Int. Symposium on Safety, Security, and Rescue Robotics*, pp. 134–142, Nov. 2011.

[12] A. M. Johnson and D. E. Koditschek, "Toward a vocabulary of legged leaping," *IEEE Int. Conf. on Robotics and Automation*, 2013.

[13] S. Kim, J. E. Clark, and M. R. Cutkosky, "iSprawl: Design and Tuning for High-speed Autonomous Open-loop Running," *The Int. Jnl. of Robotics Research*, vol. 25, no. 9, pp. 903–912, Sep. 2006.

[14] N. J. Kohut, K. C. Peterson, D. Zarrouk, and R. S. Fearing, "Aerodynamic Steering of a 10 cm High-Speed Running Robot," *IEEE Int. Conf. on Intelligent Robots and Systems*, 2013.

[15] A. McClung, J. G. Cham, and M. R. Cutkosky, "Rapid maneuvering of a biologically inspired hexapedal robot," *IMECE*, 2004.

[16] C. Ordonez, N. Gupta, E. G. Collins, J. E. Clark, and A. M. Johnson, "Power modeling of the XRL hexapedal robot and its application to energy efficient motion planning," *CLAWAR*, no. 118, pp. 689–696, 2012.

[17] A. Pullin, N. J. Kohut, D. Zarrouk, and R. S. Fearing, "Dynamic turning of 13 cm robot comparing tail and differential drive," *IEEE Int. Conf. on Robotics and Automation*, pp. 5086–5093, 2012.

[18] M. Reinstein and M. Hoffmann, "Dead reckoning in a dynamic quadruped robot: Inertial navigation system aided by a legged odometer," *IEEE Int. Conf. on Robotics and Automation*, 2011.

[19] U. Saranli, M. Buehler, and D. E. Koditschek, "RHex: A Simple and Highly Mobile Hexapod Robot," *The International Journal of Robotics Research*, vol. 20, no. 7, pp. 616–631, Jul. 2001.

[20] S. N. Sponberg, A. J. Spence, C. H. Mullens, and R. J. Full, "A single muscle's multifunctional control potential of body dynamics for postural control and running." *Philosophical transactions of the Royal Society of London. Series B, Biological sciences*, vol. 366, no. 1570, pp. 1592–605, May 2011.

[21] D. Zarrouk and R. S. Fearing, "Compliance-based dynamic steering for hexapods," *2012 IEEE/RSJ International Conference on Intelligent Robots and Systems*, pp. 3093–3098, Oct. 2012.